


First-passage distributions of an asymmetric noisy voter model

Santosh Kudtarkar*

Centre for Mathematical Modelling, FLAME University, Pune 412115, India (Received 17 November 2023; revised 29 January 2024; accepted 5 February 2024; published 28 February 2024)

This paper explores the first-passage times in an asymmetric noisy voter model through analytical methods. The noise in the model leads to bistable behavior, and the asymmetry arises from heterogeneous rates for spontaneous switching. We obtain exact analytical expressions for the probability distribution for two different initial conditions, first-passage times for switching transitions and first return times to a stable state for all system sizes, offering a deeper understanding of the model's dynamics. Additionally, we derive exact expressions for the mean switching time, mean return time, and their mean square variants. The findings are verified through numerical simulations. To enhance clarity regarding the model's behavior, we also provide approximate solutions, emphasizing the parameter dependence of first-passage times in the small switching parameter regime. An interesting result in this regime is that while the mean switching time in the leading order is independent of system size, the mean return time depends inversely on system size. This study not only advances our analytical understanding of the asymmetric noisy voter model but also establishes a framework for exploring similar phenomena in social and biological systems where the noisy voter model is applicable.

DOI: [10.1103/PhysRevE.109.024139](https://doi.org/10.1103/PhysRevE.109.024139)**I. INTRODUCTION**

The methods of statistical physics have been applied beyond its primary field and span such diverse areas as biology and societal phenomena [1]. The Voter Model (VM) [2] provides a simple framework to understand the complex dynamics underlying diverse processes in society and nature which broadly deals with the emergence of consensus [3]. Some prominent examples include the spread of ideas in a population, the emergence of consensus in a group, political opinion formation, genetics, language competition, and field-theoretic phenomena in various systems, among many others [4–9]. The agents in the VM form a complex network, and the network structure gives rise to interesting dynamics. In such models, the individuals are represented by nodes and connected by edges. In simple models, each type of agent (individual) can be in two states (+1 or –1) representing a binary opinion space in the context of opinion dynamics or a choice between two parties in the context of politics. At each time step, a randomly selected agent interacts with a randomly selected neighbor (an agent connected by an edge), and the agent may copy the state of the other. The complex networks or graphs underlying voter models range from regular lattices [2] to more complex topologies such as small-world networks [10,11], power-law degree distributions [3,12–14], multilayer networks [15–17], graphs with community-structure [18,19], and simplicial complexes, among others [20].

Voter models are restricted to not just binary states, but one can generalize the model to include n different choices. In finite VMs, consensus is the eventual fate of the system. However, this is far from reality. Different opinions can

coexist, or relationships or bonds may change over time. VMs have been modified to include different versions of reality [21]. For instance, in adaptive voter models (aVMs), pairs of agents with contradicting opinions are selected, and either both agents agree on the same opinion or they break their relationship and form a new bond with some other agent. This results in a dynamic reconfiguration of the network leading to interesting dynamics [22,23]. In the nonlinear VMs, the rate of copying depends nonlinearly on the number of agents of the other type [24]. As an example, in q -voter models (qVM), the state of an agent is flipped if the opinions of q neighboring agents are the same, else the agent changes their opinion at some constant rate [25]. In addition to models where every agent has the potential to change their states, there can also be models where a fraction of the agents called “zealots” zealously defend and hold on to their beliefs and are immune from the influence of their neighbors [26,27]. Similarly, one can introduce “contrarians” who take on the opposite view of their neighbors [28–30]. The inclusion of “zealots” and “contrarians” disrupts the system's symmetry and influences the equilibrium properties of the system. These variants can capture different phenomena, such as polarization, consensus, fragmentation, or oscillations [29–34].

Another VM variant with more realistic dynamics is the Noisy Voter Model. In these types of models the opinions of individuals can be influenced not only by their neighbors but also by external noise on individual states, leading to shifts in their own beliefs over time irrespective of the opinions of their neighbors [7,31,34–44]. These types of models take into account external influences from the environment and display finite-size phase transitions. When the noise term is stronger than the interaction term, the distribution of opinions is unimodal, indicating a coexisting of opinions, and when the noise term is weaker than the interaction term, the distribution

*sant@flame.edu.in

is bimodal, indicating consensus being the dominant behavior with relatively rare switching behavior between the two consensus states [35]. An important characteristic of noise-induced bistability is that it does not manifest at the mean-field (deterministic) level but is instead brought about by fluctuations [45]. In these instances, a singular stable state at the mean-field level transforms into bistability characterized by a bimodal probability distribution due to the influence of noise [32,37,46–49], particularly in scenarios involving small population numbers. Instances of noise-induced bistability can also be observed in ant foraging colonies, where they organize into two groups corresponding to different food sources [35,48], in the schooling behavior of fish [50], dynamics of percolation in strongly correlated systems [51], and chemical catalytic processes [47,52].

A variant of the noisy voter model is the asymmetric voter model [31,32,39]. The asymmetry arises from the heterogeneous rates of flipping for each agent type due to external stimuli, and we motivate this in the context of a noisy voter model with zealots [31]. Previous works have focused on calculating the mean switching time (MST) for the system to flip from one consensus state to the other ([44,48,49]) or its steady-state properties [31]. In this work, we study the asymmetric voter model and derive the probability distribution and the first-passage time distributions analytically. The first-passage time refers to the duration it takes for an individual's opinion to change or reach a particular state for the first time. Studying the first-passage time distribution in the Noisy Voter Model allows us to explore fundamental questions associated with the dynamics of opinion formation [53]. For instance, one can study the role of noise in shaping the emergence of consensus, the influence of initial conditions on the first-passage time, the mean time for consensus to emerge, the persistence of the system to remain in the same state, and the probability distribution of the system to return to the same state for the first time. We seek answers to these questions to gain analytical insights into the underlying mechanisms of opinion dynamics by explicitly deriving their dependence on the system's parameters. The current work employs a model similar to the one discussed in [31,32], where the authors analyze the noisy model with zealots both analytically and numerically, specifically focusing on the steady state (long-time limit) across various parameter values. Their study primarily investigates the phase changes associated with alterations in these parameters during the steady state. In contrast, our work not only utilizes the discrete master equation [54] to derive the analytical expression of the probability distribution for all time points but also extends the analysis to include the first-passage probability distributions. The steady-state properties can be easily inferred by taking the $t \rightarrow \infty$ limit of the probability distribution. We provide analytical derivations for the long-time and small-time limits, as well as mean first-passage times, enriching the understanding of the system dynamics presented in this paper. The results derived illuminate the interplay of the external noise parameters on the underlying dynamics of consensus formation and its destruction in the whole temporal regime. This work stands out for utilizing a precise framework, distinct from previous approaches that employed the approximate Fokker-Planck equation (as demonstrated, for example, in [55]) to derive the

first-passage distribution. Unlike prior methods, our approach is exact and applicable across all system sizes, as demonstrated in this paper.

This paper is organized as follows. In Sec. II we define the asymmetric noisy model by introducing zealots and susceptible agents in the VM and define the master equation for the stochastic dynamics. Section III discusses the solution of the master equation using a series expansion for two different initial conditions. Section IV presents the theoretical framework and mathematical formalism used to calculate the first-passage time distribution for the system to switch from one consensus state to the other and derive its expression using Laplace transforms. We also discuss the long- and small-time limit of the first-passage switching distribution (FPSD) and derive its mean switching time (MST) and the mean square switching time (MSST). In Sec. V we describe the mathematical formalism for the first-passage return distribution (FPRD) (the persistence distribution) for the system to return to the same state. We also derive the small- and long-time limits, the exact expression of the mean return time (MRT), and the mean square return time (MSRT). In both sections, we validate the results derived with numerical solutions. Section VI provides a discussion of the key findings, and finally concluding remarks along with directions for future work are provided in Sec. VII. Some of the mathematical details are covered in the Appendixes.

II. MODEL AND THE MASTER EQUATION

The Voter Model consists of N_T agents who can interact with any other agent in the network. The agents can be in one of two states or holding one of two opinions, **A** and **B**, leading to two subpopulations. The agents can change their opinion by interacting with other agents in the following manner:



Here Eq. (1) represents an agent of type **A** interacting with an agent of type **B** and convincing them to change their opinion at a rate \tilde{r} . Similarly Eq. (2) denotes an agent of type **B** interacting with an agent of type **A** and convincing them to change their opinion at the same rate \tilde{r} . The Noisy Voter Model introduces additional stochastic dynamics where the agents can spontaneously change their state to the other type at rate ϵ as



This corresponds to symmetric switching from **A** to **B** and vice versa where the transition rates are equal corresponding to spontaneous switching independent of agent type. One can generalize this to include asymmetric switching rates where the switching of **A** to **B** happens at the rate ϵ_1 while the switching rate from **B** to **A** is given by ϵ_2 . It is denoted as a reaction in the following manner:



We will now motivate the origin of the asymmetric switching rates in the asymmetric Noisy Voter Model by introducing “zealots” who are agents immune to changing their opinion [30,31]. Agents of each type (**A** or **B**) can again be segregated into two types: susceptible agents who can change their opinion and zealots who do not. Let $N_{A(B)}$ be the number of susceptible agents of types **A(B)** and $z_{A(B)}$ be the number of zealots of the corresponding types. The total population is then given by $N_T = N_A + z_A + N_B + z_B$. An increase in the number of agents of type **A** can come about by the reaction given in Eq. (1) along with the reverse reaction of Eq. (3). Similarly, the reactions given by Eq. (2) combined with the forward reaction of Eq. (3) lead to an increase in the number of agents of type **B**. We denote the transition rate for an increase in agents of type **A** by $W^+(n)$ and the transition rate for the decrease in agents of type **A** or equivalently the increase in agents of type **B** by $W^-(n)$. Using the standard law of mass action methodology [54] the transition rates are given by

$$W^+(n) = \tilde{r} \frac{(N_A + z_A) N_B}{N_T} + \epsilon N_B, \quad (5)$$

$$W^-(n) = \tilde{r} \frac{N_A (N_B + z_B)}{N_T} + \epsilon N_A, \quad (6)$$

where we have made use of the property that only the susceptible agents can change their type, and while zealots cannot change their type, they can influence and recruit the agents of the other type to be like them [30]. We normalize \tilde{r}/N_T to be equal to 1 without any loss of generality. The transition rates can now be rewritten in terms of redefined variables in a simpler form,

$$W^+(n) = n(N - n) + \epsilon_1(N - n), \quad (7)$$

$$W^-(n) = n(N - n) + \epsilon_2 n, \quad (8)$$

where we have defined $\epsilon_1 = \epsilon + z_A$, $\epsilon_2 = \epsilon + z_B$ and for simplicity we define $N_A + N_B = N$ and $N_A = n$, which implies $N_B = N - n$. The structural formulation of these equations reveals that the inclusion of zealots in the model introduces modifications that manifest as altered system dynamics. Specifically, the impact of zealots is captured by the existence of asymmetrical random fluctuations ($\epsilon_1 \neq \epsilon_2$ whenever $z_A \neq z_B$), which allow agents to spontaneously change their opinions at a rate that depends on their type.

The dynamics of the system is governed by the master equation, which determines the probability distribution of finding n susceptible agents holding opinion **A** (equivalently, $N - n$ susceptible agents holding opinion **B**) at time t and is given by [54]

$$\frac{dP_n(t|n_0)}{dt} = W^+(n-1)P_{n-1}(t|n_0) + W^-(n+1)P_{n+1}(t|n_0) - [W^+(n) + W^-(n)]P_n(t|n_0), \quad (9)$$

where $P_n(t|n_0) \equiv P(n, t|n_0, t_0)$ is the conditional probability for the system to be found with n agents with opinion **A** at time t given that the system started with n_0 agents at time t_0 . We solve the master equation in the next section.

The mean number of agents $\langle n \rangle = \sum_{n=0}^N n P_n(t|n_0)$ holding opinion **A** can be deduced from the master equation by multiplying both sides with n and summing from $n = 0$ to N [54].

The resulting equation is given by

$$\frac{d\langle n \rangle}{dt} = \langle W^+(n) - W^-(n) \rangle = \epsilon_1 N - (\epsilon_1 + \epsilon_2) \langle n \rangle. \quad (10)$$

Here the angular brackets $\langle \dots \rangle$ denote the mean or expectation value corresponding to the probability distribution $P_n(t|n_0)$. In the long-time limit ($t \rightarrow \infty$), the mean number of agents in the stationary state, $\langle n \rangle_s$, is given by

$$\langle n \rangle_s = \frac{\epsilon_1}{\epsilon_1 + \epsilon_2} N. \quad (11)$$

As evident from the above equation, when $\epsilon_{1(2)} = 0$, which occurs when $\epsilon = 0$ and $z_{A(B)} = 0$, the stable states of the system are either at $n = 0$ or $n = N$ and correspond to the absorbing states of the standard Voter Model [1]. This implies that in the long-time limit, the population exclusively comprises agents of type **A** or **B** indicating a consensus state. In the limit of small switching rates ($\epsilon_{1(2)} \ll 1$), the $n = 0$ and $n = N$ states cease to be absorbing but become metastable. Hence, it is reasonable to infer that the system is more likely to be situated near the boundary ($n = 0$ or $n = N$), which are metastable states rather than the state given by Eq. (11). This is a critical aspect of the dynamics of the noisy voter model where the bimodality of the distribution for small $\epsilon_{1(2)}$ is not captured in the mean-field limit but is noise-induced, which requires a stochastic treatment to understand the dynamics of the model [31,47,49]. A detailed discussion follows in Sec. VI.

III. SOLUTION OF THE MASTER EQUATION

The master equation (9) is a system of differential equations for each value of n whose exact solutions are difficult to obtain except in the simplest of cases. A useful technique that reduces the master equation and converts it into a single linear partial differential equation is the method of a probability-generating function [54]. This transformation is useful to obtain exact solutions in one-step reaction processes where for each interaction or reaction the number of agents changing their type is not more than one. These types of interactions have been well studied in stochastic gene networks and are the most preferred technique to obtain probability distributions analytically [56]. The probability-generating function is defined as $\Psi^{(n_0)}(s, t) = \sum_{n=0}^N s^n P(n, t|n_0, t_0)$ with the summation limited to the finite system size N . Multiplying both sides of the master equation (9) by s^n , summing from $n = 0$ to $n = N$ and redefining the terms in terms of the generating function, we arrive at the transformed master equation in terms of the probability-generating function $\Psi^{(n_0)}(s, t)$ which is given by

$$\begin{aligned} \frac{\partial \Psi^{(n_0)}(s, t)}{\partial t} = & (1-s)[N(1-s) + (s\epsilon_1 + \epsilon_2)] \frac{\partial \Psi^{(n_0)}(s, t)}{\partial s} \\ & - (1-s) \left\{ (1-s) \frac{\partial}{\partial s} \left[s \frac{\partial \Psi^{(n_0)}(s, t)}{\partial s} \right] \right. \\ & \left. + \epsilon_1 N \Psi^{(n_0)}(s, t) \right\}. \end{aligned} \quad (12)$$

To solve the above equation, we use the separation of variables method in s and t by expanding the probability-generating

function as a series in the eigenfunctions of the PDE [57]. This is given by

$$\Psi^{(n_0)}(s, t) = \sum_{m=0}^N C_m^{(n_0)} \psi_m^{(n_0)}(s) e^{\lambda_m t}. \quad (13)$$

Here λ_m is the m th eigenvalue corresponding to the eigenfunction $\psi_m^{(n_0)}(s)$ and $C_m^{(n_0)}$ are expansion coefficients that depend on the initial conditions. To compute the solution, it is convenient to expand the eigenfunction itself as a polynomial series in $(1-s)$ [49],

$$\psi_m^{(n_0)}(s) = \sum_{k=0}^N b_k^m (1-s)^k, \quad (14)$$

where b_k^m are the series coefficients which have to be determined. Using $1-s$ for the series expansion gives us a one-term recursion in b_k^m , instead of the multiterm one we would get by expanding in a series in s . Substituting the above in Eq. (12) and applying reflecting boundary conditions, we can solve for the eigenvalues λ_m and series coefficients b_k^m . After some algebra, we obtain the expression for the eigenvalue to be

$$\lambda_m = -m(m-1 + \epsilon_1 + \epsilon_2), \quad (15)$$

and the coefficients b_k^m are given by the recurrence relation,

$$\begin{aligned} b_k^k &= 1, \\ b_{k+1}^m &= \frac{(k-N)(k+\epsilon_1)}{\lambda_m + (k+1)(k+\epsilon_1 + \epsilon_2)} b_k^m \quad \text{for } m \leq k < N, \\ b_k^m &= 0 \quad \text{for } k < m. \end{aligned} \quad (16)$$

Following some algebraic manipulation, the above recurrence relation can be solved for b_k^m explicitly and is found to be

$$b_k^m = \begin{cases} (-1)^{k-m} \binom{N-m}{k-m} \frac{(\epsilon_1+m)_{k-m}}{(\epsilon_1+\epsilon_2+2m)_{k-m}} & m \leq k < N \\ 0 & \text{otherwise} \end{cases}. \quad (17)$$

Here $\binom{n}{k}$ are binomial coefficients and $(x)_n = x(x+1)(x+2) \cdots (x+n-1)$ denotes the Pochhammer symbol [58]. Although it is possible to calculate the probability distribution for any initial condition n_0 , this paper focuses on two specific boundary states, $n_0 = 0$ and $n_0 = N$. In the subsequent subsections, we derive an explicit expression for these two cases.

A. Probability distribution with initial condition $n_0 = 0$

We now solve for the expansion coefficients $C_m^{(n_0)}$ in Eq. (13) for the case where the system at the beginning has only zealots holding opinion **A** and zero susceptible agents of the same type ($n_0 = N_A = 0$ and $N_B = N$) at time $t_0 = 0$. This initial condition can be represented mathematically as

$$P_n(t=0|0) = P(n, 0|0, 0) = \delta_{n,0}, \quad (18)$$

where $\delta_{n,0}$ is the Kronecker delta function. This condition fixes the probability-generating function $\Psi^0(s, t)$ to take the value 1 at time $t = 0$,

$$\Psi^{(0)}(s, 0) = \sum_{m=0}^N C_m^{(0)} \sum_{k=m}^N b_k^m (1-s)^k = 1. \quad (19)$$

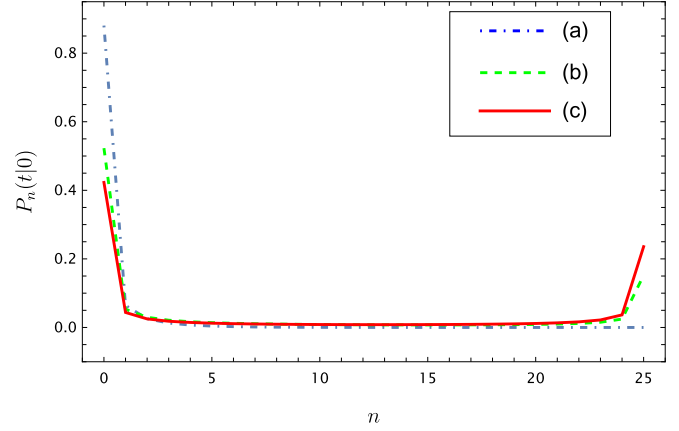


FIG. 1. Probability distribution $P_n(t|0)$ for times (a) $t = 0.1$ (---), (b) $t = 5$ (- -), (c) $t = 500$ (—) with $\epsilon_1 = 0.10$, $\epsilon_2 = 0.15$, and $N = 25$.

By noting that the above equation has to be true for any value of s , we substitute $s = 0$ to get the following system of equations:

$$\Psi^{(0)}(0, 0) = \sum_{m=0}^N C_m^{(0)} \sum_{k=m}^N b_k^m = 1 = \sum_{k=0}^N \sum_{m=0}^k C_m^{(0)} b_k^m, \quad (20)$$

where we have used the triangular property for double sums in the last expression. Using the property $b_k^k = 1$ and fixing $C_0 = 1$, the above set of equations simplifies to

$$\sum_{m=0}^k C_m^{(0)} b_k^m = 0, \quad 1 \leq k \leq N. \quad (21)$$

This is a triangular system of linear equations in $C_m^{(0)}$. Substituting Eq. (17) for b_k^m , the equations can be solved by repeated substitution leading to the following solution:

$$C_m^{(0)} = \binom{N}{m} \frac{(\epsilon_1)_m}{(\epsilon_1 + \epsilon_2 + m - 1)_m}. \quad (22)$$

Having determined b_k^m and $C_m^{(0)}$, the probability distribution of the model starting from the initial condition $n_0 = 0$ can be calculated from the probability-generating function using the following property [54]

$$P_n(t|n_0) = \frac{1}{n!} \left. \frac{\partial^n \Psi^{(0)}(s, t)}{\partial s^n} \right|_{s=0}. \quad (23)$$

Differentiating the generating function n times, the probability distribution $P_n(t|0)$ is then exactly given by the following expression:

$$P_n(t|0) = (-1)^n \sum_{m=0}^N C_m^{(0)} \sum_{j=m}^N \binom{j}{n} b_j^m e^{\lambda_m t} \quad (24)$$

with the values of C_m and b_j^m as determined above. The plot of the exact time-dependent probability distribution for the initial condition considered here is plotted in Fig. 1 for different values of $\epsilon_{1(2)}$ and time t .

A special case is the stationary probability distribution which is obtained by taking $t \rightarrow \infty$ in Eq. (24). Doing so, it can be noted that the nonzero contribution comes from only

the $m = 0$ term corresponding to the zero eigenvalue. The stationary probability distribution, $P_s(n)$, is given by

$$P_s(n) = \lim_{t \rightarrow \infty} P_n(t|0) = \binom{N}{n} \frac{(\epsilon_1)_n (\epsilon_2)_{N-n}}{(\epsilon_1 + \epsilon_2)_N}. \quad (25)$$

It is to be noted that the final steady-state distribution is independent of the initial condition.

B. Probability distribution with initial condition $n_0 = N$

We now solve for the generating function $\Psi^{(N)}(s, t)$ by determining the expansion coefficients $C_m^{(N)}$ in the converse scenario of the previous subsection wherein all the susceptible agents are only of type **A** ($N_A = n_0 = N$ and $N_B = 0$) and none of the susceptible agents are of type **B**. The initial probability distribution is given by

$$P_n(t = 0|N) = P(n, 0|N, 0) = \delta_{n,N}. \quad (26)$$

The generating function $\Psi^{(N)}(s, t)$ at time $t = 0$ should then be equal to

$$\Psi^{(N)}(s, 0) = \sum_{m=0}^N C_m^{(N)} \sum_{k=m}^N b_k^m (1-s)^k = s^N. \quad (27)$$

To solve the above equations for $C_m^{(N)}$, it is convenient to define $1 - s = y$, and the summation term in the above equation becomes

$$\sum_{k=0}^N \sum_{m=0}^k C_m^{(N)} b_k^m y^k = (1-y)^N = \sum_{k=0}^N \binom{N}{k} (-1)^k y^k. \quad (28)$$

Here we have used the triangular property for double sums and in the last equation, we have expanded $(1-y)^N$ as a binomial series in y . The final system of equations can be obtained by comparing the coefficients of the k th power of y on both sides of the above equation, which results in the following system of equations:

$$\sum_{m=0}^k C_m^{(N)} b_k^m = (-1)^k \binom{N}{k}, \quad 0 \leq k \leq N, \quad (29)$$

whose solution is obtained by repeated substitution and is given by

$$C_0^{(N)} = 1, \quad C_m^{(N)} = (-1)^m \binom{N}{m} \frac{(\epsilon_2)_m}{(\epsilon_1 + \epsilon_2 + m - 1)_m}. \quad (30)$$

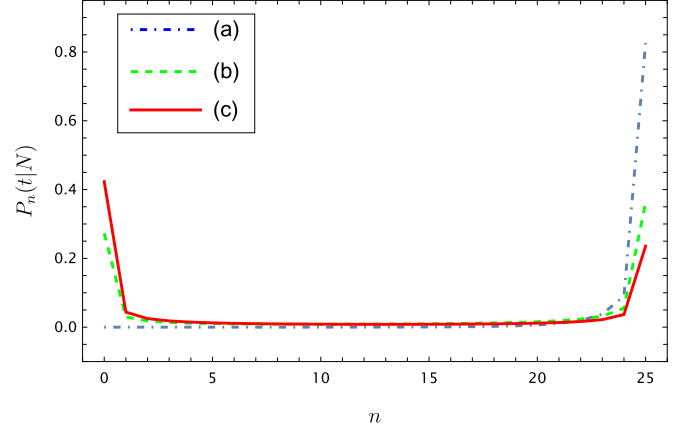


FIG. 2. Probability distribution $P_n(t|N)$ for times (a) $t = 0.1$ ($-\cdot-\cdot-$), (b) $t = 5$ ($-$), (c) $t = 500$ (red). $\epsilon_1 = 0.10$, $\epsilon_2 = 0.15$, and $N = 25$.

The probability distribution $P_n(t|N)$ is then given by the following expression:

$$P_n(t|N) = (-1)^n \sum_{m=0}^N C_m^{(N)} \sum_{j=m}^N \binom{j}{n} b_j^m e^{\lambda_m t}. \quad (31)$$

The plot of the exact time-dependent probability distribution for the initial condition considered here is plotted in Fig. 2 for various values of $\epsilon_{1(2)}$ and time t .

IV. FIRST-PASSAGE SWITCHING DISTRIBUTION

The first-passage switching distribution (FPSD) denoted by $\rho(t|n_0)$ for the system to switch from $n = 0$ to $n = N$ can be calculated from the probability distribution derived in the previous section using the method of renewal processes ([53,54]). Towards this, we consider the probability $P_N(t|0)$ of being found in the state $n = N$ starting from state $n = 0$. It can be obtained by calculating the probability, $\rho(t'|0)$, of reaching the state $n = N$ for the first time at t' , and having reached there, calculating the probability $P_N(t - t'|N)$ to be found in the state N in the remaining time $t - t'$ and integrating over all possible times t' . Mathematically, it can be represented by the convolution integral,

$$P_N(t|0) = \int_0^t dt' \rho(t'|0) P_N(t - t'|N). \quad (32)$$

In the above equation, $P_N(t|0)$ can be obtained by substituting $n = N$ in Eq. (24), which after some manipulations results in the following expression:

$$P_N(t|0) = \sum_{m=0}^N (-1)^m \binom{N}{m} \frac{(\epsilon_1)_N}{(\epsilon_1 + \epsilon_2 + m)_N} \frac{\epsilon_1 + \epsilon_2 + 2m - 1}{\epsilon_1 + \epsilon_2 + m - 1} e^{\lambda_m t} = \sum_{m=0}^N a_m e^{\lambda_m t}. \quad (33)$$

Similarly, the expression for $P_N(t|N)$ is obtained by substituting $n = N$ in Eq. (31) and is given by

$$P_N(t|N) = \sum_{m=0}^N \binom{N}{m} \frac{(\epsilon_2)_m (\epsilon_1 + m)_{N-m}}{(\epsilon_1 + \epsilon_2 + m)_N} \frac{\epsilon_1 + \epsilon_2 + 2m - 1}{\epsilon_1 + \epsilon_2 + m - 1} e^{\lambda_m t} = \sum_{m=0}^N b_m e^{\lambda_m t}. \quad (34)$$

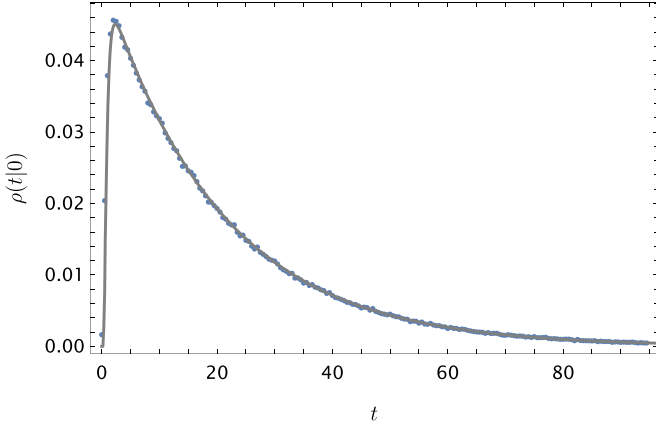


FIG. 3. Comparison of exact first-passage switching distribution (FPSD) with Monte Carlo simulations (\cdot) for $\epsilon_1 = 0.05$, $\epsilon_2 = 0.01$, and $N = 50$.

For notational convenience, we have abbreviated the coefficient of $e^{\lambda_m t}$ in the previous two expressions as a_m and b_m .

Equation (32) is an integral equation that has to be solved for $\rho(t|0)$, and the convolutional structure of the equation suggests the use of Laplace transforms to find the solution [53]. The Laplace transformed equation is given by

$$\tilde{\rho}(s|0) = \mathcal{L}(\rho(t|0)) = \frac{\tilde{P}_N(s|0)}{\tilde{P}_N(s|N)} = \frac{\sum_{m=0}^N \frac{a_m}{s+|\lambda_m|}}{\sum_{m=0}^N \frac{b_m}{s+|\lambda_m|}}, \quad (35)$$

where \mathcal{L} denotes the Laplace transform. s is the Laplace variable in the context of Laplace transforms, $|\lambda_m|$ is the absolute value of the eigenvalue, and \tilde{P}_N denotes the Laplace transformed distributions. This is the exact Laplace transform of FPSD, which has to be inverted using the inverse Laplace transform (ILT) to obtain the FPSD in t space:

$$\begin{aligned} \rho(t|0) &= \mathcal{L}^{-1}(\tilde{\rho}(s|0)) = \frac{1}{2\pi i} \int_{\gamma-i\infty}^{\gamma+i\infty} \rho(s|0) e^{st} ds \\ &= \sum_{k=1}^N \text{Res}_{s \rightarrow p_k} (\tilde{\rho}(s|0) e^{st}). \end{aligned} \quad (36)$$

The previous expression denotes the sum over the residues of the Laplace transform of FPSD multiplied by the exponential term [57]. The integrand is analytic except for N simple poles p_k , which arises due to the exponential dependence of $P_N(t|N)$ on time. Except for the smallest and the largest pole which can be approximately determined, the rest of the poles have to be calculated numerically. In addition, since all the eigenvalues of the probability distribution are negative [Eq. (15)] the poles of the Laplace transform are also negative with the following property:

$$0 > p_1 \geq p_2 \geq p_3 \cdots \geq p_N. \quad (37)$$

The FPSD has been plotted in Fig. 3 for a representative value of the parameters $\epsilon_{1(2)}$ and compared with Monte Carlo simulations. The shape of the distribution for other parameter values is qualitatively the same. In the following subsection, we will calculate the small- and long-time limits of the FPS analytically.

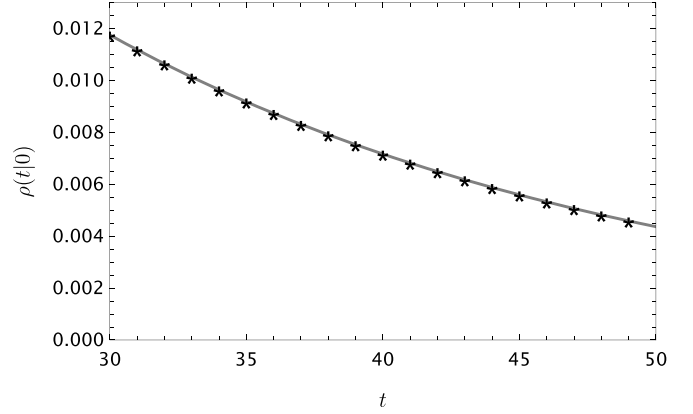


FIG. 4. Comparison of the exact first-passage switching distribution (—) with the long-time limit [Eq. (39)] (*) for $\epsilon_1 = 0.05$, $\epsilon_2 = 0.01$, and $N = 50$.

A. Long-time limit of the first-passage switching distribution

The long-time behavior ($t \gg 1$) can be calculated by taking the $s \ll 1$ limit from the Laplace transform of FPSD [Eq. (35)]. As can be seen in Eq. (36) in the limit of $s \ll 1$, the leading contribution comes from the residue at the pole, which has the largest value, p_1 . This pole can be determined by expanding $\tilde{\rho}(s|0)$ in the small- s limit. It can be seen in Eq. (35) that the poles are the zeros of $\tilde{P}_N(s|N)$ and p_1 can be determined in the small- s limit by expanding it in a series in s and solving for its roots. This is found to be

$$p_1 \approx -\frac{b_0 |\lambda_1|}{b_0 + |\lambda_1| \sum_{k=1}^N \frac{b_k}{|\lambda_k|}}. \quad (38)$$

Substituting it in Eq. (36) and keeping only the residue at p_1 , we get the following expression for the long-time limit of the FPSD:

$$\rho(t|0) \xrightarrow{t \gg 1} \text{Res}_{s \rightarrow p_1} \left(\frac{\tilde{P}_N(s|0)}{\tilde{P}_N(s|N)} \right) e^{p_1 t}. \quad (39)$$

The residue is computed at $s = p_1$, yielding the predominant term in the FPSD. A comparison of the exact distribution with the above expression in the long-time limit is shown in Fig. 4 and shows good agreement in the relevant regime.

From the small- s limit, we can obtain the moments of the FPSD, in particular, the mean switching time (MST), which is the first moment of the FPSD, and mean square switching time (MSST), which is the second moment of the FPSD [54]. To obtain these values, we use the series property of the Laplace transform to be a generator of the moments of the probability distribution. The coefficients of the series expansion in s give the corresponding moments,

$$\int_0^\infty \rho(t|0) e^{-st} dt = 1 + s \langle T \rangle_S + \frac{s^2}{2} \langle T^2 \rangle_S + O(s^3), \quad (40)$$

where

$$\langle T \rangle_S = \int_0^\infty t \rho(t|0) dt, \quad (41)$$

$$\langle T^2 \rangle_S = \int_0^\infty t^2 \rho(t|0) dt \quad (42)$$

TABLE I. Comparison of Monte Carlo simulation (prefix: Sim) and exact results (prefix: Exact) of the mean return time (MST) and mean square switching time (MSST). We have taken $N = 50$, and the number of trials for the simulation is 10^6 .

ϵ_1	ϵ_2	Sim- $\langle T \rangle_S$	Sim- $\langle T^2 \rangle_S$	Exact- $\langle T \rangle_S$	Exact- $\langle T^2 \rangle_S$
0.05	0.01	21.17	858.72	21.15	855.49
0.05	1.1	110.53	24 223.58	110.63	24 240.71
1.1	0.05	1.57	3.45	1.57	3.4433
1.1	1.5	9.11	154.12	9.09	153.53

are the first (MST) and second moments (MSST) of FPSD. Expanding the Laplace transform given by Eq. (35) in a Taylor series around $s = 0$ and retaining terms of order s and $s^2/2$ we get

$$\langle T \rangle_S = \frac{1}{a_0} \sum_{k=1}^N \frac{b_k - a_k}{|\lambda_k|}, \quad (43)$$

$$\langle T^2 \rangle_S = \frac{2}{a_0^2} \left[a_0 \sum_{k=1}^N \frac{b_k - a_k}{|\lambda_k|^2} - \left(\sum_{k=1}^N \frac{b_k}{|\lambda_k|} \right) \left(\sum_{k=1}^N \frac{a_k}{|\lambda_k|} \right) + \left(\sum_{k=1}^N \frac{b_k}{|\lambda_k|} \right)^2 \right]. \quad (44)$$

These expressions are exact and compare very well with numerical simulations as shown in Table I.

While the above expressions are exact, the complexity of the expressions hide the parameter dependence of these quantities. To obtain simple and explicit formulas, we now derive the expression for MST in the physically relevant small parameter regime of switching from the metastable state $n = 0$ to $n = N$. This can be obtained by taking the limit $\epsilon_{1(2)} \ll 1$ of Eq. (43) and is derived in Appendix A. The small parameter limit of MST is given by

$$\langle T \rangle_S \approx \frac{1}{\epsilon_1} \left(1 + \frac{N-1}{N} (\epsilon_1 + \epsilon_2) \right), \quad (45)$$

where we have ignored terms of $O(\epsilon_1^2, \epsilon_2^2, \epsilon_1 \epsilon_2, \frac{\epsilon_{1(2)}}{N})$.

B. Small-time limit of the first-passage switching distribution

The small-time limit ($t \ll 1$) of the FPSD can be obtained in the Laplace transformed space in the large s limit ($s \gg 1$). To calculate this, we consider the large s expansion of $\tilde{P}_N(s|0)$ defined in Eq. (35). It is given by

$$\tilde{P}_N(s|0) = \frac{1}{s} \sum_{k=0}^N a_k \sum_{j=0}^{\infty} \left(-\frac{|\lambda_k|}{s} \right)^j. \quad (46)$$

The above sum is derived in Appendix B and is given by

$$\sum_{k=0}^N a_k |\lambda_k|^j = \begin{cases} 0 & j < N \\ (-1)^N N! (\epsilon_1)_N & j = N, \\ N! (\epsilon_1)_N g(\epsilon_1, \epsilon_2, N) & j > N \end{cases} \quad (47)$$

where $g(\epsilon_1, \epsilon_2, N)$ is a function of ϵ_1, ϵ_2 and can be ignored in the small-time limit that is of interest in this section. Similarly, expanding $\tilde{P}_N(s|N)$, which is the denominator of Eq. (35), in the same way gives to the leading order $\tilde{P}_N(s|N) = 1$. To

obtain this, we have made use of the property $\sum_{k=0}^N b_k = 1$, which follows from the initial condition $P_N(t = 0|N) = 1$. The Laplace transformed FPSD [Eq. (35)] in the large- s limit is then given by

$$\tilde{\rho}(s|0) \approx \frac{1}{s^N} N! (\epsilon_1)_N \quad \text{when } s \gg 1. \quad (48)$$

Taking its inverse Laplace transform, we get the small-time limit of the FPSD:

$$\rho(t|0) = \mathcal{L}^{-1}[\tilde{\rho}(s|0)] = N (\epsilon_1)_N t^{N-1}, \quad (49)$$

which is a polynomial in time of order $N - 1$.

V. FIRST-PASSAGE RETURN DISTRIBUTION

In this section we derive the first passage return distribution (FPRD) for the system's return to the initial boundary state for the first time after exiting the state. Given that we have already computed the probability $P_N(t|N)$ in Eq. (31), which gives the likelihood of being in state N at time t after starting from the same state, we use the state $n = N$ as the reference to calculate FPRD. We formulate the equation governing the FPRD by observing that $P_N(t|N)$ can be expressed as a sum of probabilities as

$$P_N(t|N) = \sum_{i=0}^{\infty} P_N^{(i)}(t), \quad (50)$$

where $P_N^{(i)}(t)$ is the probability that the system is in state $n = N$ after visiting this state exactly i times by time t . In particular, $i = 0$ corresponds to the system not having left the initial state, i.e., the survival probability, which is given by (see Appendix C) for the derivation

$$P_N^{(0)}(t) \equiv S(t) = e^{-N\epsilon_2 t}. \quad (51)$$

We now write the expression for $P_N^{(1)}(t)$, which is the probability for the system to have returned to the state N after exactly one exit. This is given by

$$P_N^{(1)}(t) = \int_0^t S(t-t_2) \left[\int_0^{t_2} dt_1 L(t_1) F(t_2-t_1) \right] dt_2. \quad (52)$$

This is a double convolution integral where $L(t)$ represents the probability of the system departing from the state $n = N$ by time t , defined as $L(t) = -dS(t)/dt$. $F(t)$ denotes the probability of the system's return to the state for the first time by time t , which is precisely the first-passage return distribution (FPRD). The inner integral above denotes the probability of finding the system in state N at time t_2 following a single exit and the subsequent return. Following this return, $S(t)$ denotes the probability of remaining in the state $n = N$ without any further exits. The structure of Eq. (52) is that of a double convolution and can be represented using the standard notation for convolutions as

$$P_N^{(1)}(t) = [(L * F) * S](t), \quad (53)$$

where $*$ denotes the convolution operation. Continuing with the same reasoning, we can represent the probability $P_N^{(i)}(t)$ in terms of multiple $i + 1$ -fold convolutions as

$$P_N^{(i)}(t) = [(L * F)^i * S](t). \quad (54)$$

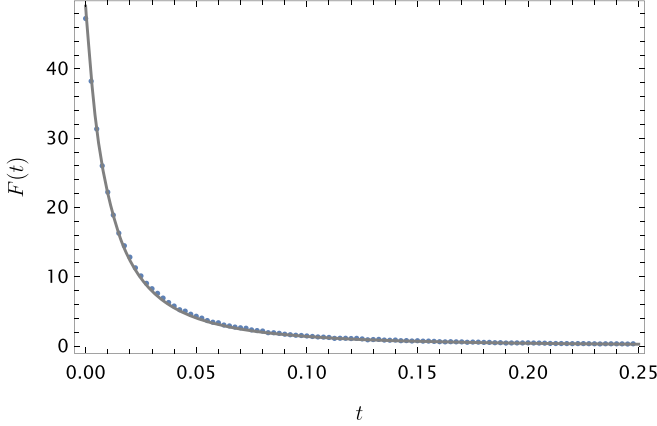


FIG. 5. Comparison of exact first-passage return probability distribution (FPRD) with Monte Carlo simulations (\cdot) for $\epsilon_1 = 0.05$, $\epsilon_2 = 0.01$, and $N = 50$.

Using this expression, Eq. (50) can then be written as

$$P_N(t|N) = S(t) + \sum_{i=1}^{\infty} [(L * F)^i * S](t). \quad (55)$$

This equation has to be solved for $F(t)$, which is the FPRD. Due to its convolutional nature, Laplace transforms are a convenient method of solution. Taking the Laplace transform of both sides of the equation we obtain

$$\tilde{F}(s) = \frac{1}{\tilde{L}(s)} \left(1 - \frac{\tilde{S}(s)}{\tilde{P}_N(s|N)} \right), \quad (56)$$

where as mentioned earlier the \sim symbol on the functions denotes the Laplace transforms. Substituting the expressions for $\tilde{S}(s)$, $\tilde{L}(s)$, and $P_N(s|N)$, the expression for $\tilde{F}(s)$ can be obtained and is given by

$$\tilde{F}(s) = \frac{(s+d)}{d} - \frac{s}{d(b_0 + \sum_{m=1}^N \frac{s b_m}{s + |\lambda_m|})}, \quad (57)$$

where we have defined $d = N\epsilon_2$. Similar to the case of the FPSD, we can use the inverse Laplace transform to invert the above equation to obtain the FPRD distribution. It can be noted that the poles of $\tilde{F}(s)$ are the same as the poles of $\tilde{\rho}(s|0)$ and occur at the zeros of $\tilde{P}_N(s|N)$, which are denoted by p_k . The FPRD is then given by

$$F(t) = \sum_{k=1}^N \text{Res}_{s \rightarrow p_k} [\tilde{F}(s)e^{st}]. \quad (58)$$

In Fig. 5 we plot the FPRD for a specific value of the parameter $\epsilon_{1(2)}$ and compare it with results obtained by Monte Carlo simulations. The qualitative nature of FPRD remains the same for different parameter values.

A. Long-time limit of the first-passage return distribution and the mean return time

Similar to the procedure employed for finding the long-time limit of FPSD in Sec. IV A, the Laplace transform of $F(t)$ given in Eq. (57) can be inverted in the limit of $s \rightarrow 0$ to obtain the long-time limit of FPRD. In this limit, the dominant pole

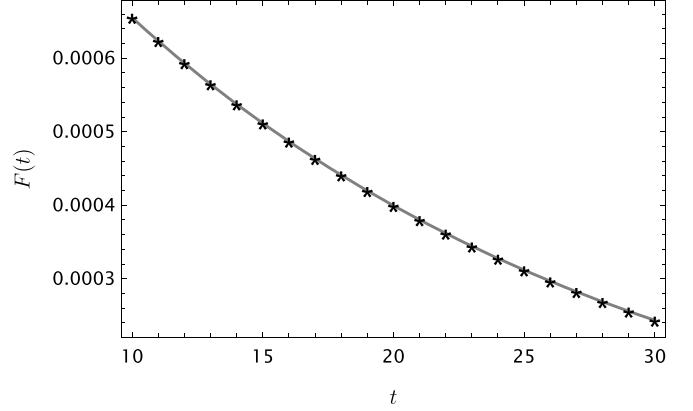


FIG. 6. Comparison of the exact first-passage return distribution (—) with the expression of the long-time limit [Eq. (59) (*) for $\epsilon_1 = 0.05$, $\epsilon_2 = 0.01$, and $N = 50$.

is given by the smallest absolute value of the pole of $\tilde{P}_N(s|N)$, which has been obtained earlier in Eq. (38). The long-time limit is determined by the first term of the sum in Eq. (58), which is given by

$$F(t) = \frac{p_1^2(p_1 + |\lambda_1|)}{db_0|\lambda_1|} e^{p_1 t}. \quad (59)$$

This is a good approximation in the small parameter limit. The comparison between the actual distribution and the long-time approximation is given in Fig. 6 and shows excellent agreement validating the goodness of the approximation. Similar to the first-passage switching distribution (FPSD), this also exhibits exponential decay in the long-time limit with the same rate constant p_1 .

The mean return time (MRT) and the mean square return time (MSRT) can be obtained by expanding $\tilde{F}(s)$ in the small s limit. This series is given by

$$\int_0^{\infty} F(t)e^{-st} dt = 1 + s\langle T \rangle_R + \frac{s^2}{2}\langle T^2 \rangle_R + O(s^3), \quad (60)$$

where $\langle T \rangle_R$ and $\langle T^2 \rangle_R$ are the MRT and MSRT of $F(t)$ and are defined similarly to the MST and MSST. Using similar methods given in Sec. IV A, the following expressions for MRT and MSRT are obtained:

$$\langle T \rangle_R = \frac{1}{N\epsilon_2} \left(\frac{1}{b_0} - 1 \right), \quad (61)$$

$$\langle T^2 \rangle_R = \frac{2}{b_0^2 N \epsilon_2} \sum_{i=1}^N \frac{b_i}{|\lambda_i|}, \quad (62)$$

where $b_0 = (\epsilon_1)_N / (\epsilon_1 + \epsilon_2)_N$. These results have been validated with Monte Carlo simulations and show good agreement as shown in Table II.

The mean return time (MRT) in the limit of $\epsilon_{1(2)} \ll 1, N \gg 1$ can be derived using methods similar to those used in the limit of and MST as given in Appendix A,

$$\langle T \rangle_R \approx \frac{\{1 + (\epsilon_2 + 2\epsilon_1)[\gamma + \log(N)]\}}{N\epsilon_1}, \quad (63)$$

where γ is the Euler constant.

TABLE II. Comparison of Monte Carlo simulation (prefix: Sim) and exact results (prefix: Exact) of the mean return time (MRT) and mean square return time (MSRT). We have taken $N = 50$, and the number of trials for the simulation is 500 000.

ϵ_1	ϵ_2	Sim- $\langle T \rangle_R$	Sim- $\langle T^2 \rangle_R$	Exact- $\langle T \rangle_R$	Exact- $\langle T^2 \rangle_R$
0.05	0.01	0.50	17.16	0.50	17.75
0.05	1.1	28.27	6187.32	28.10	6137.87
1.1	0.05	0.0958	0.09895	0.0963	0.0996
1.1	1.5	3.23	53.35	3.25	54.07

B. Small-time limit of the first-passage return distribution

The small-time limit of the FPRD can be obtained from $\tilde{F}(s)$ by taking the large- s ($s \gg 1$) limit. We expand Eq. (57) in a series in s around $s = \infty$ and keeping the leading two terms in the series, we get

$$\tilde{F}(s) = \frac{d_2 - d^2}{ds} + \frac{2dd_2 - d_3 - d^3}{ds^2} + O(1/s^3). \quad (64)$$

Here $d = N\epsilon_2 = \sum_{m=1}^N b_m |\lambda_m|$, $d_2 = \sum_{m=1}^N b_m |\lambda_m|^2$, and $d_3 = \sum_{m=1}^N b_m |\lambda_m|^3$. From the derivation given in Appendix D, we obtain the following formulas for the sums:

$$d_2 = d(\alpha^+ + d), \quad (65)$$

$$d_3 = d[(\alpha^+ + d)^2 + \alpha^+ \alpha^-], \quad (66)$$

where $\alpha^+ = N - 1 + \epsilon_1$ and $\alpha^- = (N - 1)(1 + \epsilon_2)$. Substituting the above in Eq. (64), we obtain

$$\tilde{F}(s) = \frac{\alpha^+}{s} - \frac{\alpha^+(\alpha^+ + \alpha^-)}{s^2} + O(1/s^3). \quad (67)$$

Taking the inverse Laplace transform, the small time limit of the FPRD is given by

$$F(t) = \alpha^+ - \alpha^+(\alpha^+ + \alpha^-)t + O(t^2). \quad (68)$$

From the above it can be inferred that unlike FPSD, the leading behavior of FPRD is a constant.

VI. DISCUSSION

We now discuss salient aspects of the results that we have derived in this paper. The time-dependent probability distribution has been precisely derived from the master equation under two distinct initial conditions, when $n_0 = 0$ and $n_0 = N$. To examine the influence of noise on this probability distribution, we focus on the long-time limit, leading to the establishment of the steady-state probability distribution. This is given in Eq. (25), which is obtained by taking the $t \rightarrow \infty$ limit of the exact probability distribution given in Eq. (24). It can be noted that the final steady-state distribution is independent of the initial condition. By studying the parameter dependence of the steady-state distribution, two regimes can be discerned: (1) unimodal when either of ϵ_1 or ϵ_2 exceeds 1.00 and (2) bimodal when both ϵ_1 and ϵ_2 fall below 1.0. The uni- or bimodal nature depends solely on the noise parameters and is independent of the system size N . In the unimodal regime, the mode is situated below $N/2$ when $\epsilon_1 < \epsilon_2$ and at $n = 0$ when $\epsilon_1 < 1 < \epsilon_2$. Conversely when $\epsilon_1 > \epsilon_2$, the

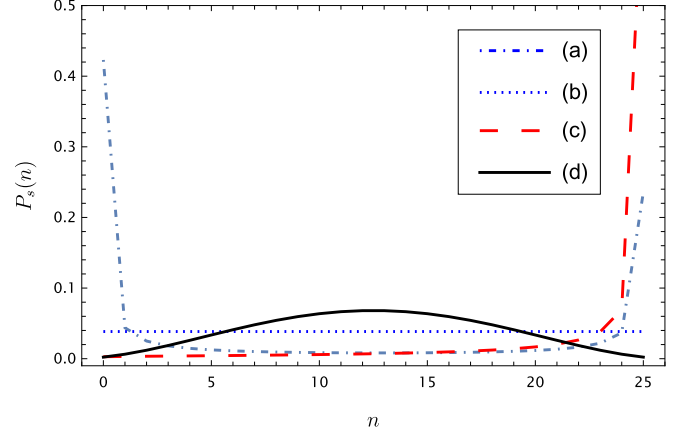


FIG. 7. Comparison of the steady-state probability distribution for (a) $\epsilon_1 = 0.1, \epsilon_2 = 0.15$ ($\cdot \cdot \cdot$) (b) $\epsilon_1 = 1.1, \epsilon_2 = 0.1$ ($-$), (c) $\epsilon_1 = 1.0, \epsilon_2 = 1.0$ ($\cdot \cdot \cdot$), and (d) $\epsilon_1 = 3.1, \epsilon_2 = 3.1$ (thick line).

mode is located above $N/2$ and in particular at $n = N$ when $\epsilon_2 < 1 < \epsilon_1$. Symmetry is achieved with the mode precisely at $N/2$ when $\epsilon_1 = \epsilon_2 > 1$, signifying an equal likelihood for either opinion to be held. Conversely, the bimodal regime has peaks at $n = 0$ and $n = N$, which take equal values when $\epsilon_1 = \epsilon_2$. A special case arises when $\epsilon_1 = \epsilon_2 = 1$. Substituting this in Eq. (25) results in a constant probability distribution given by $P_s(n) = \frac{1}{N+1}$ [49]. This indicates a phase transition from an unimodal to a bimodal state when both transition rates cross the threshold of 1. The steady-state probability distribution, depicted in Fig. 7, illustrates both unimodal and bimodal states across a range of parameter values. In the context of opinion dynamics, the unimodal distribution represents the coexistence of opinions **A** and **B**, when both $\epsilon_{1(2)} > 1$ and the bimodal denotes the fixation of one opinion indicating consensus. The dependence on parameters of the unimodal and bimodal phases reveals two interesting paths to a phase transition, namely, (1) by changing the noise term ϵ and/or (2) from the definition of $\epsilon_{1(2)}$, by changing the number of zealots within the population.

Using the expression of the exact probability distribution we have established renewal equations to compute the distribution of first-passage times which represents the time taken by the system to transition entirely from one consensus state to another (FPSD). This is given in Eq. (36) using the residues of the Laplace transform. To examine the parameter dependence, we have analyzed the long-time [Eq. (39)] and small-time limits [Eq. (49)] of FPSD. Notably, in the asymptotic regime, the leading behavior of the long-time limit is characterized by an exponential function, with the rate constant p_1 given by Eq. (38). It can be demonstrated that in the small parameter limit ($\epsilon_{1(2)} \ll 1$), $p_1 \approx -\epsilon_1$ and $\rho(t|0) \propto e^{-\epsilon_1 t}$, signifying that the switching dynamics from $n = 0$ to $n = N$ in the long term is governed by a relatively slow drop off due to the smallness of ϵ_1 . The small-time limit has been similarly derived and is given by Eq. (49), which reveals the polynomial dependence on time, namely, $\rho(t|0) \propto t^{N-1}$ when $t \ll 1$. The constant of proportionality however scales rapidly with system size N . This is exact for any system size. To enable comparison with the behavior obtained from Fokker-Planck equations, which is

the continuum limit of the master equation, one can take the large N and small t limit keeping Nt constant. Equation (49) then becomes

$$\rho(t|0) = \frac{\sqrt{2\pi}}{\Gamma(\epsilon_1)} \frac{1}{t^{\epsilon_1 + \frac{3}{2}}} e^{-\frac{1}{t}}, \quad (69)$$

where we have made use of the asymptotic properties of the Pochhammer symbol in the limit of $N \gg 1$ and $\Gamma(n)$ denotes the gamma function [58]. The negative exponential dependence on inverse time as $t \rightarrow 0$ and the time-dependent power-law behavior are distinctive features of first-passage probabilities within the Fokker-Planck framework [55]. However, the $-3/2$ power-law dependence in the Fokker-Planck framework is modified to $-(\epsilon_1 + 3/2)$, which has been derived using the exact formalism presented in this paper. In the limit of $\epsilon_1 \ll 1$, the power-law dependence agrees with the Fokker-Planck formalism.

We now discuss the small parameter dependence of the mean-switching time (MST) from the metastable state $n = 0$ to $n = N$ given in Eq. (45). It can be noticed in the limit of $\epsilon_1 \ll 1$, the primary contribution to the mean switching time (MST) is inversely proportional to the switching parameter ϵ_1 and remains unaffected by the system size N , viz, $\langle T \rangle_S \sim 1/\epsilon_1$. Importantly, it is only in the subleading term that N emerges, and this dependence on N becomes irrelevant for $N \gg 1$. This suggests that under small noise conditions, the MST exhibits constancy as a function of system size as its leading behavior.

We now consider the first-passage return distribution (FPRD). It exhibits exponential dependence with the same rate constant as that of the first-passage switching (FPSD) distribution in the long-time limit [compare Eq. (39) with Eq. (59)], i.e., $F(t) \propto e^{-\rho_1 t}$. However, it is in the small-time limit that they differ significantly. While the FPSD vanishes at time $t = 0$, FPRD takes a nonzero value $F(0) = N - 1 + \epsilon_1$ which depends on both system size N and ϵ_1 . An interesting aspect to note here is that like in the case of MST, the leading order behavior is inversely proportional to ϵ_1 but unlike MST, it is inversely proportional to the size of the system N , namely, $\langle T \rangle_R \sim 1/(N\epsilon_1)$. This reveals that the MRT is not only affected by system size, but the larger its value the lower the time taken on average to the return to the initial metastable state.

VII. CONCLUSION

In conclusion, the stochastic dynamics of opinion formation within a diverse population have been the focus of our investigation into the first-passage dynamics of an asymmetric noisy voter model with heterogeneous switching rates. Our analytical approach is rooted in the exact solution of the master equation for all values of the system size N and helps in unraveling the behavior of the system. The bimodal and unimodal behavior exhibited by the model has a significant influence on the switching transitions between opinion states. The derivation of the first-passage switching and return distributions across various parameter regimes has revealed the presence of the exponential distribution in the long-time limit.

The quantitative aspects of the asymmetric voter model have been elucidated by the exact derivation of the mean

switching and return times (MST and MRT) and mean square switching and return times (MSST and MSRT). Notably, the MST's inverse proportionality to the noise parameter and its independence of the system size in the small parameter limit for large systems underscores the universality of the phenomena of dependence on noise. This finding implies that the time required for the system to transition between opinion states is primarily governed by the switching rate (noise), which is an interesting aspect that enhances the understanding of the temporal aspects of the noisy voter model. In addition, the mean return time (MRT) has shown an inverse relationship between the noise parameter and the system size. This stands in stark contrast to the almost size-independent nature of the MST.

The methods employed in this paper have been validated through Monte Carlo simulations. The findings hold implications for sociophysics and biophysics. The ability to model opinion dynamics in populations with heterogeneous switching rates is not only pertinent to understanding social networks' evolution but also bears relevance to biological systems providing a broader understanding of complex systems. The analytical framework and the exact results derived in this paper open avenues for exploring more complex scenarios, incorporating additional parameters and opinion states to model real-world contexts analytically. For instance, one can explore the effect of external influences, such as media or influential individuals on opinion dynamics or the inclusion of multiple opinion states effect the system's behavior. While we have studied the complete network where interactions between agents are long-ranged, it would be interesting to study the dynamics of asymmetric noise in the context of short-range interactions. Addressing these questions and expanding the scope of our model could offer deeper insights into the underlying mechanisms governing opinion dynamics in heterogeneous populations.

ACKNOWLEDGMENTS

Partial funding from the Roop Manek Bhanshali Trust (Project No. RES/EXT/2022/0182) is gratefully acknowledged.

APPENDIX A: MEAN SWITCHING TIME IN THE SMALL PARAMETER LIMIT

The exact expression for the mean switching time (MST) is given in Eq. (43),

$$\langle T \rangle_S = \sum_{m=1}^N \left(\frac{b_m - a_m}{a_0} \right) \frac{1}{|\lambda_m|}, \quad (A1)$$

where

$$a_m = (-1)^m \binom{N}{m} \frac{(\epsilon_1)_N}{(\epsilon_1 + \epsilon_2 + m)_N} \frac{\epsilon_1 + \epsilon_2 + 2m - 1}{\epsilon_1 + \epsilon_2 + m - 1}, \quad (A2)$$

$$b_m = \binom{N}{m} \frac{(\epsilon_2)_m (\epsilon_1 + m)_{N-m}}{(\epsilon_1 + \epsilon_2 + m)_N} \frac{\epsilon_1 + \epsilon_2 + 2m - 1}{\epsilon_1 + \epsilon_2 + m - 1}, \quad (A3)$$

$$a_0 = \frac{(\epsilon_1)_N}{(\epsilon_1 + \epsilon_2)_N}. \quad (A4)$$

The small switching parameter limit ($\epsilon_1, \epsilon_2 \ll 1$) implies that $\lambda_m = -m(m-1 + \epsilon_1 + \epsilon_2)$, which appears in the denominator of Eq. (43), is greater than 1 for all $m > 1$ and is equal to $\epsilon_1 + \epsilon_2$ for $m = 1$. This results in only the first term of the sum being the dominant term of the MST and is given by

$$\langle T \rangle_S \approx \frac{N(\epsilon_1 + \epsilon_2)_N(\epsilon_1 + \epsilon_2 + 1)}{(\epsilon_1)_N(\epsilon_1 + \epsilon_2 + 1)_N((\epsilon_1 + \epsilon_2)^2)} \times [(\epsilon_1)_N + \epsilon_2(1 + \epsilon_1)_{N-1}]. \quad (\text{A5})$$

To simplify this expression, we now make use of the following two properties of the Pochhammer symbol:

$$\frac{(x)_N}{(1+x)_N} = \frac{x}{x+N} = x \left(1 - \frac{x}{N}\right) + O\left(\frac{x^3}{N^2}\right),$$

$$\frac{(1+x)_{N-1}}{(x)_N} = \frac{1}{x},$$

which are applicable in the limit of $x \ll 1$. Using these expressions and assuming that $N \gg \epsilon_1, \epsilon_2$, we arrive at the following result:

$$\langle T \rangle_S \approx \frac{1}{\epsilon_1} \left(1 + \frac{N-1}{N}(\epsilon_1 + \epsilon_2)\right) + O(\epsilon_1^2, \epsilon_2^2, \epsilon_1\epsilon_2, \frac{\epsilon_1(2)}{N}). \quad (\text{A6})$$

APPENDIX B: SUMMATION OF $\sum_{m=0}^N a_m \lambda_m^j$

The summation given in Eq. (47) can be derived by noting that

$$P_N(t|0) = \sum_{m=0}^N a_m e^{\lambda_m t}$$

$$\Rightarrow \frac{\partial^j P_N(t|0)}{\partial t^j} \Big|_{t \rightarrow 0} = \sum_{m=0}^N a_m \lambda_m^j. \quad (\text{B1})$$

We employ the initial condition $P_n(t=0|0) = \delta_{n,0}$ and repeatedly differentiate the master equation (9) multiple times to get the following identities:

$$\frac{\partial^j P_N(t|0)}{\partial t^j} \Big|_{t \rightarrow 0} = \begin{cases} 0 & 1 \leq j < N \\ \prod_{k=1}^N W^+(N-k) & j = N \end{cases}. \quad (\text{B2})$$

Using the expression for the $W^+(n)$, we obtain the result given in Eq. (47), $\prod_{k=1}^N W^+(N-k) = N!(\epsilon_1)_N$.

APPENDIX C: PROBABILITY OF SURVIVAL IN THE STATE $n = N$

The probability $S(t)$ for the system to remain in the state $n = N$ without transitions can be inferred from the master equation (9) by substituting $n = N$ and ignoring all contributions to this state from the neighboring state, namely, $P_{N-1}(t|N)$ as we are interested in the persistence of the system in state N . The resulting equation then is given by

$$\frac{dS(t)}{dt} = -N\epsilon_2 S(t). \quad (\text{C1})$$

Since we are looking at survival at least for time t , we solve the above equation in the time range from t to ∞ to obtain the

following result:

$$S(t) = e^{-N\epsilon_2 t}. \quad (\text{C2})$$

The exponential dependence of the survival time is as expected from Markov property which underlies the master equation [54].

APPENDIX D: SUMMATION OF $\sum_{m=0}^N b_m \lambda_m^j$

By differentiating j times the summation given in Eq. (34) and taking the limit $t \rightarrow 0$, we get

$$P_N(t|N) = \sum_{m=0}^N b_m e^{\lambda_m t}$$

$$\Rightarrow \frac{\partial^j P_N(t|N)}{\partial t^j} \Big|_{t \rightarrow 0} = \sum_{m=0}^N b_m \lambda_m^j. \quad (\text{D1})$$

We employ the initial condition $P_n(t=0|N) = \delta_{n,N}$ and repeatedly differentiate the master equation (9) multiple times to obtain the following recurrent system of equations:

$$\frac{\partial^j P_N(t|N)}{\partial t^j} \Big|_{t \rightarrow 0} = W^+(N-1) \frac{\partial^{j-1} P_{N-1}(t|N)}{\partial t^{j-1}} \Big|_{t \rightarrow 0}$$

$$- W^-(N) \frac{\partial^{j-1} P_N(t|N)}{\partial t^{j-1}} \Big|_{t \rightarrow 0}, \quad (\text{D2})$$

$$\frac{\partial^{j-1} P_{N-1}(t|N)}{\partial t^{j-1}} \Big|_{t \rightarrow 0} = W^-(N) \frac{\partial^{j-2} P_N(t|N)}{\partial t^{j-2}} \Big|_{t \rightarrow 0}$$

$$- [W^+(N-1) + W^-(N-1)]$$

$$\times \frac{\partial^{j-2} P_{N-1}(t|N)}{\partial t^{j-2}} \Big|_{t \rightarrow 0}. \quad (\text{D3})$$

We can recursively solve the above two equations to obtain a closed-form solution. In this paper we are interested only in the results corresponding to $j = 1, 2, 3$. The solutions are given by

$$\sum_{k=0}^N b_k \lambda_k = -d, \quad (\text{D4})$$

$$\sum_{k=0}^N b_k \lambda_k^2 = d(\alpha^+ + d), \quad (\text{D5})$$

$$\sum_{k=0}^N b_k \lambda_k^3 = -d[(\alpha^+ + d)^2 + \alpha^+ \alpha^-], \quad (\text{D6})$$

where we have defined

$$d = W^-(N) = N\epsilon_2, \quad (\text{D7})$$

$$\alpha^+ = W^+(N-1) = N-1 + \epsilon_1, \quad (\text{D8})$$

$$\alpha^- = W^-(N-1) = (N-1)(1 + \epsilon_2). \quad (\text{D9})$$

- [1] C. Castellano, S. Fortunato, and V. Loreto, Statistical physics of social dynamics, *Rev. Mod. Phys.* **81**, 591 (2009).
- [2] P. Clifford and A. Sudbury, A model for spatial conflict, *Biometrika* **60**, 581 (1973); R. A. Holley and T. M. Liggett, Ergodic theorems for weakly interacting infinite systems and the voter model, *Ann. Probab.* **3**, 643 (1975).
- [3] A. Baronchelli, C. Castellano, and R. Pastor-Satorras, Voter models on weighted networks, *Phys. Rev. E* **83**, 066117 (2011).
- [4] W. J. Ewens, *Mathematical Population Genetics I: Theoretical Introduction*, Interdisciplinary Applied Mathematics, Vol. 27 (Springer, New York, 2004).
- [5] R. A. Blythe and A. J. McKane, Stochastic models of evolution in genetics, ecology and linguistics, *J. Stat. Mech.: Theory Exp.* (2007) P07018.
- [6] E. Ben-Naim, L. Frachebourg, and P. L. Krapivsky, Coarsening and persistence in the voter model, *Phys. Rev. E* **53**, 3078 (1996).
- [7] J. Fernández-Gracia, K. Suchecki, J. J. Ramasco, M. San Miguel, and V. M. Eguíluz, Is the voter model a model for voters?, *Phys. Rev. Lett.* **112**, 158701 (2014).
- [8] P. L. Krapivsky, Kinetics of monomer-monomer surface catalytic reactions, *Phys. Rev. A* **45**, 1067 (1992).
- [9] I. Dornic, H. Chaté, J. Chave, and H. Hinrichsen, Critical coarsening without surface tension: The universality class of the voter model, *Phys. Rev. Lett.* **87**, 045701 (2001).
- [10] C. Castellano, D. Vilone, and A. Vespignani, Incomplete ordering of the voter model on small-world networks, *Europhys. Lett.* **63**, 153 (2003).
- [11] D. Vilone and C. Castellano, Solution of voter model dynamics on annealed small-world networks, *Phys. Rev. E* **69**, 016109 (2004).
- [12] V. Sood and S. Redner, Voter model on heterogeneous graphs, *Phys. Rev. Lett.* **94**, 178701 (2005).
- [13] K. Suchecki, V. M. Eguíluz, and M. San Miguel, Voter model dynamics in complex networks: Role of dimensionality, disorder, and degree distribution, *Phys. Rev. E* **72**, 036132 (2005).
- [14] H.-X. Yang, W.-X. Wang, Z.-X. Wu, Y.-C. Lai, and B.-H. Wang, Diversity-optimized cooperation on complex networks, *Phys. Rev. E* **79**, 056107 (2009).
- [15] S. Boccaletti, G. Bianconi, R. Criado, C. I. del Genio, J. Gómez-Gardenes, M. Romance, I. Sendina-Nadal, Z. Wang, and M. Zanin, The structure and dynamics of multilayer networks, *Phys. Rep.* **544**, 1 (2014).
- [16] M. Diakonova, V. Nicosia, V. Latora, and M. San Miguel, Irreducibility of multilayer network dynamics: The case of the voter model, *New J. Phys.* **18**, 023010 (2016).
- [17] F. Battiston, M. Perc, and V. Latora, Determinants of public cooperation in multiplex networks, *New J. Phys.* **19**, 073017 (2017).
- [18] X. Castelló, R. Toivonen, V. M. Eguíluz, J. Saramäki, K. Kaski, and M. San Miguel, Anomalous lifetime distributions and topological traps in ordering dynamics, *Europhys. Lett.* **79**, 66006 (2007).
- [19] N. Masuda, Voter model on the two-clique graph, *Phys. Rev. E* **90**, 012802 (2014).
- [20] L. Horstmeyer and C. Kuehn, Adaptive voter model on simplicial complexes, *Phys. Rev. E* **101**, 022305 (2020).
- [21] S. Redner, Reality-inspired voter models: A mini-review, *C. R. Phys.* **20**, 275 (2019).
- [22] G. C. M. A. Ehrhardt, M. Marsili, and F. Vega-Redondo, Phenomenological models of socioeconomic network dynamics, *Phys. Rev. E* **74**, 036106 (2006).
- [23] P. Holme and M. E. J. Newman, Nonequilibrium phase transition in the coevolution of networks and opinions, *Phys. Rev. E* **74**, 056108 (2006).
- [24] J. Cox and R. Durrett, Nonlinear voter models, in *Random Walks, Brownian Motion, and Interacting Particle Systems: A Festschrift in Honor of Frank Spitzer*, edited by R. Durrett and H. Kesten (Birkhauser, Boston, MA, 1991), pp. 189–201.
- [25] C. Castellano, M. A. Muñoz, and R. Pastor-Satorras, Non-linear q -voter model, *Phys. Rev. E* **80**, 041129 (2009).
- [26] M. Mobilia, Does a single zealot affect an infinite group of voters?, *Phys. Rev. Lett.* **91**, 028701 (2003).
- [27] M. Mobilia, A. Petersen, and S. Redner, On the role of zealotry in the voter model, *J. Stat. Mech.: Theory Exp.* (2007) P08029.
- [28] S. Galam, Contrarian deterministic effects on opinion dynamics: “The hung elections scenario”, *Physica A* **333**, 453 (2004).
- [29] N. Masuda, Voter models with contrarian agents, *Phys. Rev. E* **88**, 052803 (2013).
- [30] N. Khalil and R. Toral, The noisy voter model under the influence of contrarians, *Physica A* **515**, 81 (2019).
- [31] N. Khalil, M. San Miguel, and R. Toral, Zealots in the mean-field noisy voter model, *Phys. Rev. E* **97**, 012310 (2018).
- [32] N. Khalil and T. Galla, Zealots in multistate noisy voter models, *Phys. Rev. E* **103**, 012311 (2021).
- [33] A. Vendeville, B. Guedj, and S.-M. Zhou, Towards control of opinion diversity by introducing zealots into a polarised social group, in *Complex Networks & Their Applications X: Volume 2, Proceedings of the Tenth International Conference on Complex Networks and Their Applications COMPLEX NETWORKS 2021* (Springer Nature, Switzerland AG, 2022), pp. 341–352.
- [34] F. Herreras-Azcué and T. Galla, Consensus and diversity in multistate noisy voter models, *Phys. Rev. E* **100**, 022304 (2019).
- [35] A. Kirman, Ants, rationality, and recruitment, *Q. J. Econ.* **108**, 137 (1993).
- [36] B. L. Granovsky and N. Madras, The noisy voter model, *Stochastic Proc. Appl.* **55**, 23 (1995).
- [37] T. Biancalani, T. Rogers, and A. J. McKane, Noise-induced metastability in biochemical networks, *Phys. Rev. E* **86**, 010106(R) (2012).
- [38] A. Carro, R. Toral, and M. San Miguel, The noisy voter model on complex networks, *Sci. Rep.* **6**, 24775 (2016).
- [39] A. F. Peralta, A. Carro, M. San Miguel, and R. Toral, Analytical and numerical study of the non-linear noisy voter model on complex networks, *Chaos* **28**, 075516 (2018).
- [40] A. F. Peralta, A. Carro, M. S. Miguel, and R. Toral, Stochastic pair approximation treatment of the noisy voter model, *New J. Phys.* **20**, 103045 (2018).
- [41] L. Rozanova and M. Boguñá, Dynamical properties of the herding voter model with and without noise, *Phys. Rev. E* **96**, 012310 (2017).
- [42] A. Kononovicius, Supportive interactions in the noisy voter model, *Chaos Solitons Fractals* **143**, 110627 (2021).

- [43] R. Martinez-Garcia, C. López, and F. Vazquez, Species exclusion and coexistence in a noisy voter model with a competition-colonization tradeoff, *Phys. Rev. E* **103**, 032406 (2021).
- [44] A. Caligiuri and T. Galla, Noisy voter models in switching environments, *Phys. Rev. E* **108**, 044301 (2023).
- [45] W. Horsthemke and R. Lefever, *Noise Induced Transitions: Theory and Applications in Physics, Chemistry, and Biology* (Springer, Berlin, 1984).
- [46] Y. Togashi and K. Kaneko, Transitions induced by the discreteness of molecules in a small autocatalytic system, *Phys. Rev. Lett.* **86**, 2459 (2001).
- [47] J. Ohkubo, N. Shnerb, and D. A. Kessler, Transition phenomena induced by internal noise and quasi-absorbing state, *J. Phys. Soc. Jpn.* **77**, 044002 (2008).
- [48] T. Biancalani, L. Dyson, and A. J. McKane, Noise-induced bistable states and their mean switching time in foraging colonies, *Phys. Rev. Lett.* **112**, 038101 (2014).
- [49] B. Houchmandzadeh and M. Vallade, Exact results for a noise-induced bistable system, *Phys. Rev. E* **91**, 022115 (2015).
- [50] J. Jhawar, R. G. Morris, U. R. Amith-Kumar, M. Danny Raj, T. Rogers, H. Rajendran, and V. Guttal, Noise-induced schooling of fish, *Nat. Phys.* **16**, 488 (2020).
- [51] J. L. Lebowitz and H. Saleur, Percolation in strongly correlated systems, *Physica A* **138**, 194 (1986).
- [52] K. A. Fichtorn, E. Gulari, and R. M. Ziff, Noise-induced bistability in a Monte Carlo surface-reaction model, *Phys. Rev. Lett.* **63**, 1527 (1989).
- [53] S. Redner, *A Guide to First-Passage Processes* (Cambridge University Press, Cambridge, 2001).
- [54] C. Gardiner, *Stochastic Methods: A Handbook for the Natural and Social Sciences* (Springer, Berlin, 2009).
- [55] O. Artime, N. Khalil, R. Toral, and M. San Miguel, First-passage distributions for the one-dimensional Fokker-Planck equation, *Phys. Rev. E* **98**, 042143 (2018).
- [56] A. M. Walczak, A. Mugler, and C. H. Wiggin, Analytic methods for modeling stochastic regulatory networks, in *Computational Modeling of Signaling Networks*, edited by X. Liu and M. Betterton, Vol. 880 (Humana Press, Totowa, NJ, 2012).
- [57] G. B. Arfken, H. J. Weber, and F. E. Harris, *Mathematical Methods for Physicists: A Comprehensive Guide*, 7th ed. (Academic Press, Waltham, MA, 2013).
- [58] M. Abramowitz and I. A. Stegun (eds.), *Handbook of Mathematical Functions with Formulas, Graphs, and Mathematical Tables*, 10th ed. (U.S. Government Printing Office, Washington, DC, 1972).